Photosystem Activity and State Transitions of the Photosynthetic Apparatus in Cyanobacterium *Synechocystis* PCC 6803 Mutants with Different Redox State of the Plastoquinone Pool

Y. V. Bolychevtseva[1]*, F. I. Kuzminov[2,3], I. V. Elanskaya[4], M. Y. Gorbunov[3], and N. V. Karapetyan[1]

[1]*Bach Institute of Biochemistry, Russian Academy of Sciences, Leninsky pr. 33,
119071 Moscow, Russia; E-mail: bolychev@inbi.ras.ru*
[2]*Faculty of Physics, Lomonosov Moscow State University, 119991 Moscow, Russia*
[3]*Department of Marine and Coastal Sciences, Rutgers, the State University of New Jersey,
New Brunswick, New Jersey 08901, USA*
[4]*Faculty of Biology, Lomonosov Moscow State University, 119991 Moscow, Russia*

Abstract—To better understand how photosystem (PS) activity is regulated during state transitions in cyanobacteria, we studied photosynthetic parameters of photosystem II (PSII) and photosystem I (PSI) in *Synechocystis* PCC 6803 wild type (WT) and its mutants deficient in oxidases (Ox⁻) or succinate dehydrogenase (SDH⁻). Dark-adapted Ox⁻ mutant, lacking the oxidation agents, is expected to have a reduced PQ pool, while in SDH⁻ mutant the PQ pool after dark adaptation will be more oxidized due to partial inhibition of the respiratory chain electron carriers. In this work, we tested the hypothesis that control of balance between linear and cyclic electron transport by the redox state of the PQ pool will affect PSII photosynthetic activity during state transition. We found that the PQ pool was reduced in Ox⁻ mutant, but oxidized in SDH⁻ mutant after prolonged dark adaptation, indicating different states of the photosynthetic apparatus in these mutants. Analysis of variable fluorescence and 77K fluorescence spectra revealed that the WT and SDH⁻ mutant were in State 1 after dark adaptation, while the Ox⁻ mutant was in State 2. State 2 was characterized by ~1.5 time lower photochemical activity of PSII, as well as high rate of P700 reduction and the low level of P700 oxidation, indicating high activity of cyclic electron transfer around PSI. Illumination with continuous light 1 (440 nm) along with flashes of light 2 (620 nm) allowed oxidation of the PQ pool in the Ox⁻ mutant, thus promoting it to State 1, but it did not affect PSII activity in dark adapted WT and SDH⁻ mutant. State 1 in the Ox⁻ mutant was characterized by high variable fluorescence and P700⁺ levels typical for WT and the SDH⁻ mutant, indicating acceleration of linear electron transport. Thus, we show that PSII of cyanobacteria has a higher photosynthetic activity in State 1, while it is partially inactivated in State 2. This process is controlled by the redox state of PQ in cyanobacteria through enhancement/inhibition of electron transport on the acceptor side of PSII.

To maintain high productivity under changing light conditions, photosynthetic organisms have adopted several mechanisms, including thermal dissipation of excess absorbed energy and dynamic adaptation of light-harvesting processes in response to light having different spectral properties and intensities [1, 2]. Photosynthetic organisms are capable of redistributing the absorbed light energy between photosystems I (PSI) and II (PSII), which is accompanied by short-term modifications in the photosynthetic apparatus organization known as "state transitions" [3-6]. This process is controlled by the redox state of the electron carriers between the photosystems [6-8]. State 1 condition is induced by light 1, driven by oxidation of the intersystem electron carriers such as the plas-

toquinone (PQ) pool and cytochrome b_6/f complex, and results in more absorbed light energy being delivered to PSII. State 2 condition is driven by reduction of PQ and cyt b_6/f under light 2 illumination and results in an increase in energy transfer to PSI.

Regulation of state transitions in cyanobacteria differs from that in plants because of the fundamental difference in their light-harvesting processes and electron transport chain organization. Photosynthetic membranes of plants and eukaryotic algae contain an integral chlorophyll *a/b* light-harvesting complex (LHCII). State transitions in these organisms are believed to result from reversible phosphorylation of these LHCII complexes that induces migration of LHCII between the PSII-enriched grana and PSI-enriched stromal membranes. LHCII phosphorylation is catalyzed by protein kinase localized in the thylakoid membrane, and this enzyme activity is controlled by the redox state of the PQ pool and/or cytochrome b_6/f complex [6-9]. Cyanobacteria contain no LHCII; instead, they employ large extra-membranous light-harvesting complexes, phycobilisomes (PBS), which deliver absorbed light energy to PSII and PSI [10-12]. Also, in contrast to eukaryotes, cyanobacteria are relatively poor in PSII compared to PSI [12, 13]. Thylakoid membranes of cyanobacteria contain both photosynthetic electron carriers (PQ, cyt b_6/f, PSI, PSII), the respiratory chain carriers (dehydrogenases NDH-1 and NDH-2 and the succinate dehydrogenase SDH) that contribute to electron transfer into the PQ pool [14-16] as well as terminal oxidases (presumably quinol oxidases) [17]. Despite these differences from eukaryotic algae and plants, cyanobacteria are also able to modify the photosynthetic apparatus depending on the redox state of the PQ pool and the cyt b_6/f complex [8, 18, 19]. Several mechanisms of PBS-absorbed energy redistribution between the photosystems in the course of state transitions have been proposed, including changes in the effective absorption cross-section of PSII and PSI as a result of PBS lateral diffusion [20, 21], changes in the aggregation of PSI (trimer−monomer) and PSII (dimer−monomer) complexes [22-25], as well as mobility of all pigment−protein complexes and spillover energy migration [26]. However, the mechanism that links changes in the redox state of electron carriers and energy migration in cyanobacteria remains unclear.

In darkness, the PQ pool in cyanobacteria is reduced by NDH-1, NDH-2, and SDH that leads to transition to State 2 [5, 8, 18, 27]. As NDH-1 dehydrogenase shows predominantly NADPH specificity [14, 28, 29], at least two pathways of cyclic electron transport involving both PQ and PSI have been reported: Fd-dependent and NDH-1-dependent [30, 31]. Many data indicate correlation between the predominant type of electron transport (linear or cyclic) and the state of the photosynthetic apparatus in both eukaryotic and prokaryotic organisms. When either NDH-1-dependent or both NDH-1- and

Fd-dependent cyclic electron transport was inhibited in mutants of *Synechococcus* PCC 7002, their photosynthetic apparatus was predominantly in State 1 after 2-min dark incubation in the presence of dichlorophenyl-dimethyl urea (DCMU) [27]. However, under anaerobic conditions or in the presence of potassium cyanide (KCN), these mutants underwent transition to State 2 [27]. The green alga *Chlamydomonas reinhardtii* is able to switch from linear to cyclic electron transport upon transition from State 1 to State 2 [32]. In State 2 with active cyclic electron transport, the reversible photoinactivation of PSII was more pronounced than in State 1 with dominant linear electron transport [33]. Acceleration of cyclic electron transport in *Synechocystis* mutants with inhibited NDH-1- or Fd-dependent electron transport was possible under high light, which was sufficient to induce PSII photoinactivation [31]. Thus, to some extent the balance between linear and cyclic electron transport might also regulate state transitions in cyanobacteria.

It was shown that the electron transport chain involving succinate dehydrogenase is the main respiratory electron transfer pathway into the PQ pool in darkness. Type I and II NDH-dehydrogenases regulate the reduction level of NADP and NAD, which, in turn, affects respiratory electron flow through succinate dehydrogenase [29]. Absence of succinate dehydrogenase decreases the flux of electrons to the PQ pool, which makes the pool more oxidized in darkness [29]. Incubation of cyanobacteria in the dark for several hours can also result in oxidized PQ pool [14, 34]. Thus, in both *Synechocystis* WT and SDH⁻ mutant, State 1 is expected after dark adaptation. In contrast, in *Synechocystis* mutant deficient in terminal oxidases (Ox⁻) the PQ pool is reduced after dark adaptation [35], thus we can expect State 2 of the photosynthetic apparatus.

To elucidate possible alterations in PSII activity during state transitions, we studied the effect of the redox state of PSII acceptors on PSII variable fluorescence in *Synechocystis* WT and its mutants SDH⁻ [16] and Ox⁻ [36], deficient in succinate dehydrogenase and terminal oxidases (CtaI, CtaII and Cyd), respectively. To induce state transitions in WT and mutants, we applied light of different quality: the phycobilisome-absorbed light (620 nm − light 2), and the light mainly absorbed by chlorophyll−protein complexes in PSI and PSII cores (440 and 680 nm − light 1). Our experiments revealed a basic difference in the initial state of the photosynthetic apparatus in the tested mutants after dark adaptation. We observed State 1 in *Synechocystis* WT and SDH⁻ mutant cells and State 2 in Ox⁻ mutant, when measurements were performed using pulsed actinic light 2 (620 nm). Under additional continuous blue illumination, all tested strains showed signs of State 1. Thus, the low yield of variable fluorescence in State 2 and its increase under additional continuous blue illumination during transition to State 1 in Ox⁻ mutant indicates partial inactivation of PSII in State 2 in cyanobacteria.

MATERIALS AND METHODS

The cells of the wild type (WT) cyanobacteria *Synechocystis* PCC 6803 and mutants Ox⁻ ($ctaCDE^-$/$cydAB^-$/$ctaDEII^-$, lacking terminal oxidases) [36] and SDH⁻ ($sll1625^-$/$sll0823^-$, lacking succinate dehydrogenase) [16] were grown photoautotrophically for 4-5 days at 30°C under continuous white light of 40 $\mu mol \cdot m^{-2} \cdot s^{-1}$. The samples were continuously stirred in liquid mineral medium BG11 [37] containing necessary antibiotics. The resulting cell cultures were collected using mild filtration on filters (Nalgene, USA; pore size 0.45 μm, sample volume 150 ml) with a Nalgene manual pump and diluted with growth medium to the required suspension density. The collected cells were kept for 1.5-2 h in darkness without stirring at room temperature, or for 30 min under light from an incandescent lamp (25-30 $\mu mol \cdot m^{-2} \cdot s^{-1}$) with slow stirring. Chlorophyll concentration was measured in 80% acetone extracts according to [38].

Fluorescence spectra at 77K were recorded using a Shimadzu RF-5301PC (Japan) spectrofluorometer in a 0.1-cm cuvette. Chlorophyll concentration in the samples was 1.5-2 μg/ml. The slit width of monochromator for exciting light (570 nm) was set to 5 nm, and the slit width of monochromator for detection of emitted light to 3 nm. Spectra were corrected to spectral sensitivity and normalized to the emission band at 722 nm.

To provide transition of the photosynthetic apparatus to State 1, the cells of *Synechocystis* in the presence of $5 \cdot 10^{-5}$ M DCMU were illuminated for 1 min with 680 or 440 nm light (70 $\mu mol \cdot m^{-2} \cdot s^{-1}$); the fluorescence was detected at room temperature using a PAM-101 pulse fluorometer (Walz, Germany) [39]. DCMU was added 2 min before measurement. A halogen lamp (KL-1500, Schott) with interference filters BPF-680 (half-passband of 35 nm; Fotooptik Ltd., Russia) or BPF-440/10 (half-passband 10 nm; Fotooptik Ltd.) was used as a source of 680 or 440 nm light, respectively.

The pulse-induced fluorescence kinetics of samples in the absence of DCMU was measured using the PAM-101 fluorometer (620 nm actinic light, 300 $\mu mol \cdot m^{-2} \cdot s^{-1}$, 1 s) with an actinic lamp (High Power LED-Lamp, control unit HPL-C) based on LEDs from Walz (Germany); the pulse-to-pulse interval was 15 s, and each average kinetic was calculated from seven sequential time courses. Additional continuous 440 nm light (70 $\mu mol \cdot m^{-2} \cdot s^{-1}$) from a halogen lamp (KL-1500) with a BPF 440/10 interference filter was used together with 620 nm actinic light flashes without preliminary illumination.

The pulse-induced absorption changes of P700 at 810 nm (relatively to 870 nm) under the same actinic illumination (620 nm, 300 $\mu mol \cdot m^{-2} \cdot s^{-1}$, 1 s) or with far-red actinic light 730 nm were recorded using an ED-P700DW dual-wavelength system (Walz) [40]. Far-red 730-nm light (4000 $\mu mol \cdot m^{-2} \cdot s^{-1}$, 1 s) was derived from the High Power LED-Lamp (control unit HPL-C) based on LEDs from Walz (Germany). The experiments were performed at chlorophyll concentration of 5 or 10 μg/ml in a 1-cm cuvette.

The intensity of far-red and 680-nm actinic light was measured using an Optical Power Meter System light power meter (Thorlabs, Germany). The intensity of 440 and 620 nm actinic light was measured using a Quantitherm quantometer (QRT1; Hansatech, Germany).

RESULTS

Cells of the Ox⁻ mutant incubated for 2 h in the dark were characterized by lower variable fluorescence yield in the presence of DCMU as opposed to the WT cells and SDH⁻ mutant (Figs. 1a and 1b). However, after 30 min exposure to white light, the WT and the two mutants showed virtually the same yield of variable fluorescence (Figs. 1c and 1d). Thus, the variable fluorescence of the WT and SDH⁻ mutant (in contrast to the variable fluorescence of Ox⁻ cells) did not change after 30-min light adaptation (Fig. 1). Similar values of variable fluorescence in all samples after light adaptation indicated the same relative content of the PSII reaction centers in these strains (Fig. 1d). Low yield of variable fluorescence for dark-adapted Ox⁻ mutant can be a sign of State 2 [41]. We used dark incubation of the investigated cultures as it provided better contrast in the variable fluorescence yield between WT and Ox⁻ mutant cells. In addition to the low variable fluorescence yield, dark-adapted Ox⁻ mutant cells had high rate of P700⁺ dark reduction ($\tau_{1/2} = 155 \pm 42$ ms) after 1 s exposure to strong far-red light (730 nm, 4000 $\mu mol \cdot m^{-2} \cdot s^{-1}$) in the presence of DCMU as compared with WT (415 $\pm$ 103 ms) and SDH⁻ mutant (416 $\pm$ 110 ms). These data indicate high rate of cyclic electron transport in the OX⁻ mutant.

It has been shown that the state of the photosynthetic apparatus depends on the redox state of the electron carriers between the photosystems [8, 18, 19]. To evaluate the redox state of the PQ pool in *Synechocystis* WT and mutant cells, we calculated the ratio of area over the time course of variable fluorescence in the presence of DBMIB and ascorbate (S_{DBMIB}) to that in the presence of DCMU (S_{DCMU}) [42]. This ratio was very low for Ox⁻ mutant cells as compared to the values obtained for WT and SDH⁻ (Fig. 2). This is in good accordance with data on high reduction level of the PQ pool in dark-adapted mutant lacking oxidases [35].

To prove State 2 of photosynthetic apparatus in dark-adapted Ox⁻ mutant cells, we compared the 77K spectra of dark-adapted cells to 77K spectra of cells illuminated with white light (30 $\mu mol \cdot m^{-2} \cdot s^{-1}$) for 30 min. In all cases, DCMU was added just before freezing. The Ox⁻ mutant shows the lowest fluorescence yield in the range of PSII fluorescence emission ($F_{692}/F_{722} = 0.94$) when compared to WT and SDH⁻ (table and Fig. 3). PSII fluorescence yield
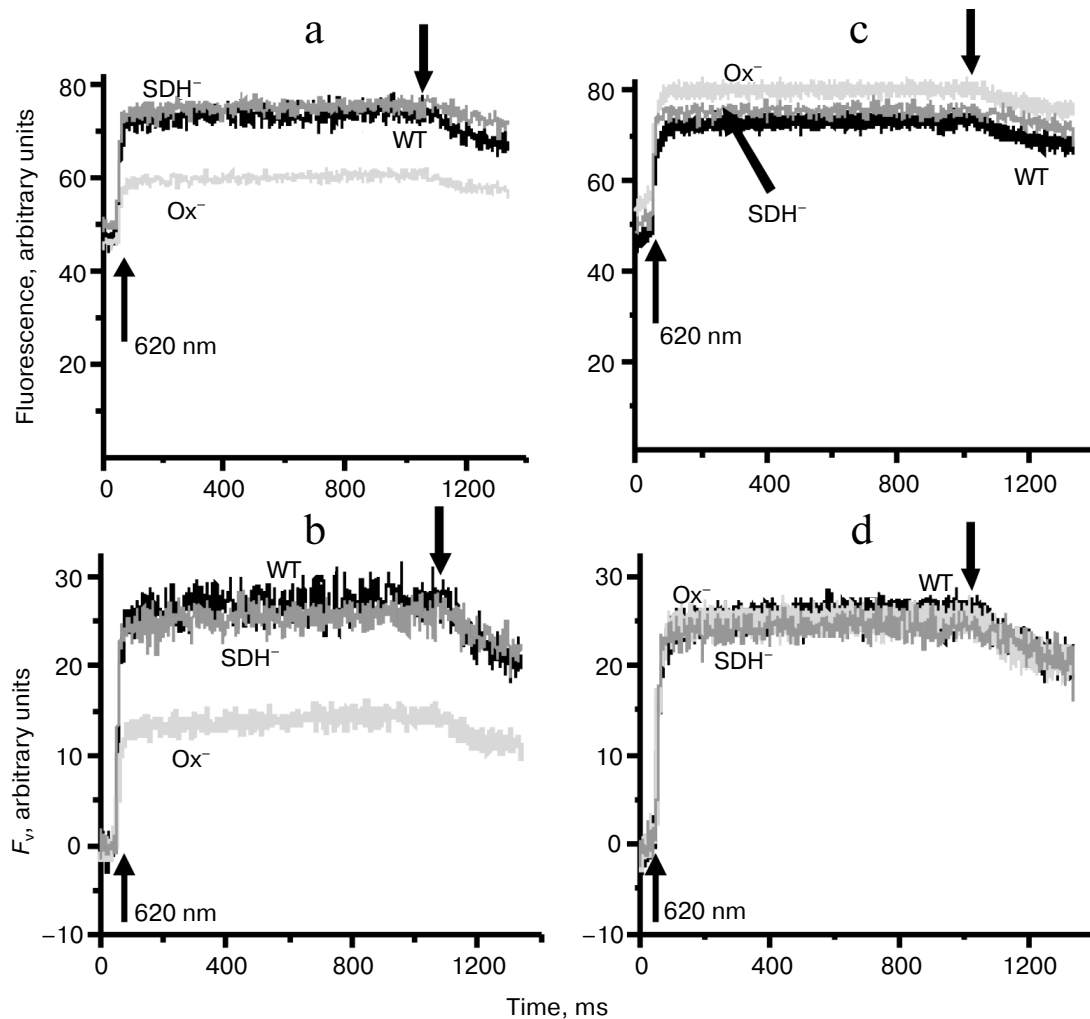
Fig. 1. Kinetics of variable fluorescence of *Synechocystis* wild-type (WT) and Ox⁻ or SDH⁻ mutant cells: (a, b) incubated in the dark for 2 h or (c, d) exposed to white light 25 μmol·m^{-2}·s^{-1} for 30 min. Measurements were made in the presence of 50 μM DCMU with actinic light of 620 nm (30 μmol·m^{-2}·s^{-1}). b, d) F_v is variable fluorescence; arrows ↑ and ↓ indicate switching actinic light on and off, respectively. Each curve represents an average of three curves obtained in three independent experiments; chlorophyll concentration, 10 μg/ml.

of the WT cells only slightly changed after illumination with white light (Fig. 3a), but it significantly increased in Ox⁻ mutant (table and Fig. 3b). The SDH⁻ mutant did not show any fluorescence yield increase in the range of PSII fluorescence emission (684 and 692 nm) (table and Fig. 3c). The increase in fluorescence level in the range of PSII fluorescence emission indicates transition of the photosynthetic apparatus from State 2 to State 1 [23, 27].

Actinic light of any spectral composition in the presence of DCMU induces reactions similar to those induced by light 1 (excitation of PSI and oxidation of PQ pool), thereby causing transition of the cyanobacterial photosynthetic apparatus to State 1 [27]. Therefore, to reveal the state of the photosynthetic apparatus in the *Synechocystis* cells incubated in the dark for 2 h, we monitored variable fluorescence of WT and mutant cells under

Ratio of 77K fluorescence yield at 692 nm (F_{692}) or 684 nm (F_{684}) to that at 722 nm (F_{722}). Data are illustrated in Fig. 3

| Incubation conditions of cells	WT		Ox⁻		SDH⁻	
	F_{692}/F_{722}	F_{684}/F_{722}	F_{692}/F_{722}	F_{684}/F_{722}	F_{692}/F_{722}	F_{684}/F_{722}
Dark, 2 h	1.03	1.06	0.94	1.20	1.29	1.19
Illumination, 30 min	1.15	1.14	1.41	1.65	1.24	1.19
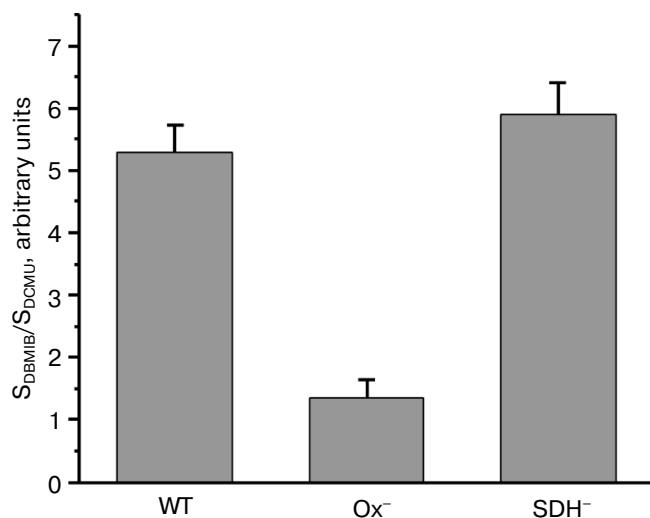
Fig. 2. Ratio of area above the curve F_V, component of variable fluorescence in the presence of 60 μM DBMIB (S_{DBMIB}), to the area above the curve F_V, component of variable fluorescence in the presence of 50 μM DCMU and 60 μM DBMIB (S_{DCMU}), calculated for *Synechocystis* cells of wild type (WT) and mutants Ox$^-$ and SDH$^-$ incubated for 2 h in the dark; bars represent mean ± s.d. of values obtained in five independent experiments.

680 nm continuous illumination in the presence of DCMU (Fig. 4). To evaluate the maximum fluorescence yield just after dark incubation of cells (F_{MD}), we applied a short flash (1 s) of saturating 620 nm light. Variable fluorescence yield of Ox$^-$ cells measured upon the first saturating 620 nm light flash (F_{MD}) in the presence of DCMU was significantly lower as compared with WT and SDH$^-$ cells. The first short flash was followed by continuous red light (680 nm), which induced a rapid increase in fluorescence to the level observed upon the first saturating flash (F_{MD}). This initial increase was followed by a gradual rise of the fluorescence that within 1 min of light treatment reached a maximum level (F_{ML}). This F_{ML} value was the same as those induced by the flash of saturating 620 nm light applied 15-20 s after the 680 nm light was turned off (Fig. 4). The WT cells of *Synechocystis* demonstrated only insignificant changes in the fluorescence yield induced by 680 nm light (Fig. 4). The phase of slow fluorescence rise in the SDH$^-$ mutant was virtually absent, and the maximum fluorescence levels prior (F_{MD}) and after (F_{ML}) 680 nm actinic light exposure were almost identical.

As the light passing through the 680-nm filter can be partially absorbed by PBS, and PBS might participate in alterations of the photosynthetic apparatus during state transitions, we performed similar measurements as shown on Fig. 4 but using 440-nm actinic light (absorbed by chlorophyll and carotenoids but not by PBS). The time courses of variable fluorescence induced by the 440-nm or 680-nm light in the WT and mutants of *Synechocystis* followed the same patterns (Fig. 5a). Despite the same changes in the photosynthetic apparatus state in the pres-

ence of DCMU induced by 440-nm light (not absorbed by PBS) and 680-nm light (partially absorbed by PBS), the latter was two times more efficient in increasing the fluorescent yield (Fig. 5b).

The state of the cyanobacterial photosynthetic apparatus could be tested using relative PSII fluorescence yield increase after exposure to light in the presence of DCMU (($F_{ML} - F_{MD}$)/F_{MD}, state transition indicator) [27]. Figure 6a shows the value of the state transition indicator ($F_{ML} - F_{MD}$)/F_{MD} and changes in parameters of PSII quantum
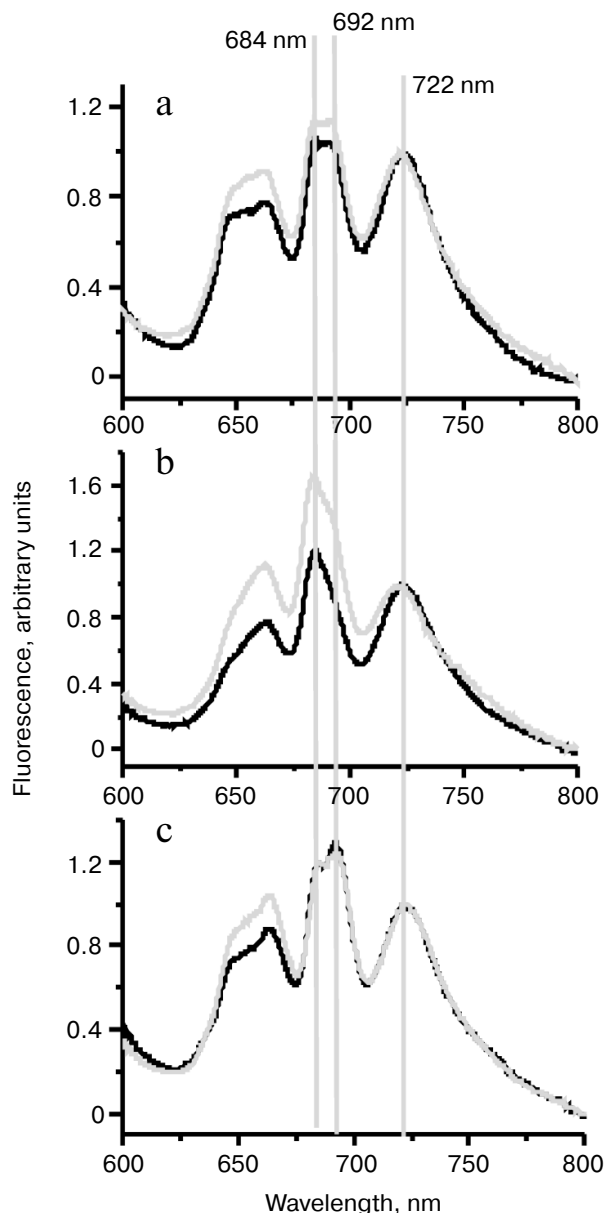
Fig. 3. Representative 77K fluorescence emission spectra of *Synechocystis* WT (a), Ox$^-$ (b), and SDH$^-$ (c) cells dark adapted (black) or after exposure to white light 25 μmol·m^{-2}·s^{-1} for 30 min (gray). Mutant cells were incubated in the dark for 2 h in the absence of DCMU, and DCMU was added to the samples before freezing to the final concentration of 50 μM. λ_{ex}, 570 nm; the spectra were normalized at 722 nm.
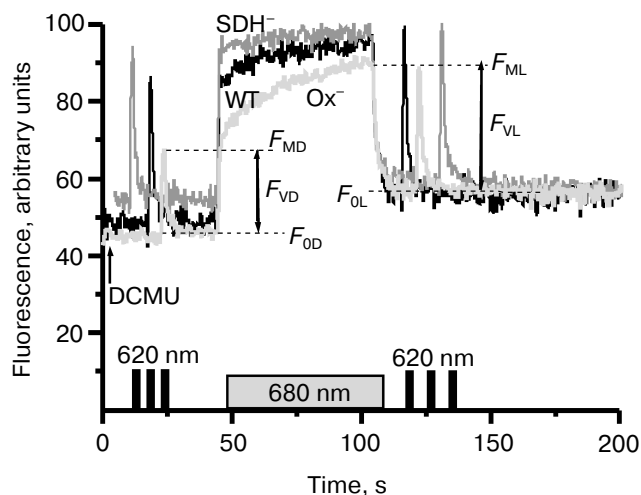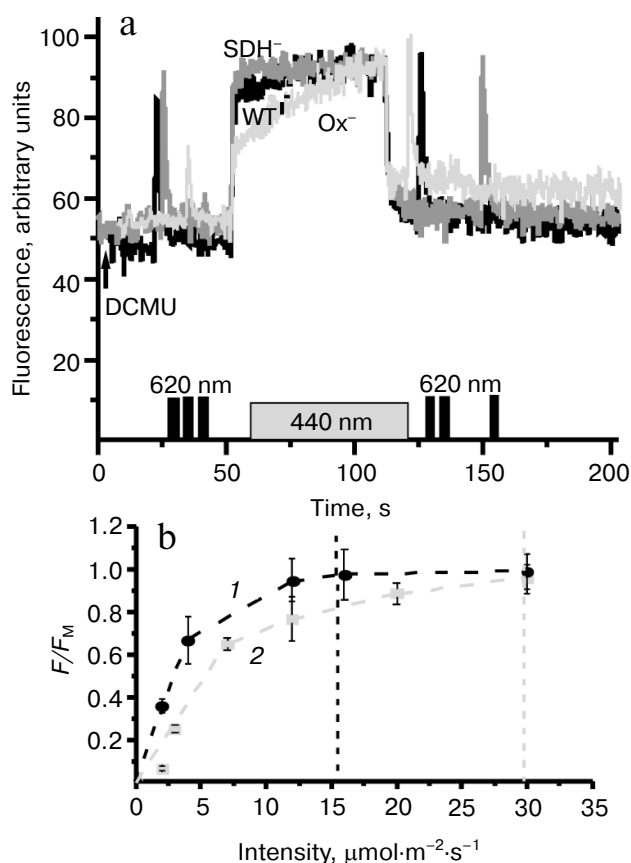
Fig. 4. Kinetic of variable fluorescence of *Synechocystis* cells of wild type (WT, black) and mutants Ox⁻ (Ox⁻, light gray) and SDH⁻ (SDH⁻, gray) after incubation in the dark for 2 h. The experiments were carried out in the presence of 50 μM DCMU; measuring light 650 nm (<1 μmol·m⁻²·s⁻¹, 1.6 kHz); actinic light 680 nm (70 μmol·m⁻²·s⁻¹, 1 min). Before and after 680 nm illumination, the cells were exposed to short (1 s) saturating flash of 620 nm light (4800 μmol·m⁻²·s⁻¹). The figures illustrate the initial (F_0), variable (F_V), and maximum (F_M) fluorescence levels before (F_{0D}, F_{VD}, F_{MD}) and after (F_{0L}, F_{VL}, F_{ML}) 680 nm illumination. Each curve represents an average of three curves obtained in three independent experiments; chlorophyll concentration, 10 μg/ml.

reduced Q_B, while phase P — to the redox state of $Q_A^- Q_B^{2-}$ and PQH_2 [43-45]. In dark-adapted Ox⁻ cells, in contrast to the WT and the SDH⁻ mutant cells, there was a decrease in the fluorescence yield just after phase J (Fig. 7a). Figure 7b shows the P700 redox reactions measured under the same experimental conditions as the fluorescence induction. The rise of I-phase fluorescence (~50 ms from the moment of turning the actinic light on) in the WT and the SDH⁻ mutant cells coincided with the onset of the re-reduction of P700⁺ during illumination, which may reflect exhaustion of the PSI acceptor, probably, because of FNR inactivation during long dark incubation of cells [46]. The rate of P700⁺ re-reduction in Ox⁻ mutant during the first 200 ms of illumination was higher than in the other cells (Fig. 7b) despite the same relative

efficiency $(F_M - F_0)/F_M$ before (D) and after (L) exposure to 680-nm light in presence of DCMU. The highest changes in the value of $(F_{ML} - F_{MD})/F_{MD}$ after exposure to 680-nm light were detected in the Ox⁻ mutant cells (Fig. 6a). These data indicated State 2 in Ox⁻ before and State 1 after illumination with light 680 nm. There was no significant difference between the quantum efficiency of PSII before and after exposure to actinic light in either mutant or WT in the presence of DCMU. It follows from Fig. 6b that the increase in the maximum fluorescence (F_M) of the Ox⁻ mutant was due to an increase in both F_0 (by 15-20%) (enhanced PBS emission in State 1) and F_V (by 50-60%), which indicated a rise of PSII activity. In the WT or SDH⁻ mutant, these effects were not observed (Fig. 6b). Thus a clear difference in PSII activity between Ox⁻ and SDH⁻ mutants (in the presence of DCMU) could indicate a difference in the functional state of PSII reaction centers after 2 h dark-adaptation period.

To evaluate the state of the PSII reaction centers in *Synechocystis* cells, we monitored pulse-induced (620 nm, 300 μmol·m⁻²·s⁻¹, 1 s) PSII fluorescence induction in the absence of DCMU (Fig. 7). Kinetics of the variable fluorescence of the Ox⁻ cells differed substantially from those of the WT and SDH⁻ mutant (Fig. 7a). The typical kinetics of variable fluorescence with second-time resolution includes phases O-J-I-P. Phase J is attributed to reduction of Q_A, which is in dynamic equilibrium with the PQ pool. Phase I corresponds to an increase in the concentration of

Fig. 5. a) Representative kinetics of the variable fluorescence of *Synechocystis* cells of wild type (WT, black) and mutants Ox⁻ (Ox⁻, light gray) and SDH⁻ (SDH⁻, gray) after incubation in the dark for 2 h. The experiments were carried out in the presence of 50 μM DCMU; measuring light 650 nm (<1 μmol·m⁻²·s⁻¹, 1.6 kHz); actinic light 440 nm (70 μmol·m⁻²·s⁻¹, 1 min). Before and after 440 nm illumination cells were exposed to short (1 s) saturating flash of 620-nm light (4800 μmol·m⁻²·s⁻¹). b) Dependence of fluorescence yield of Ox⁻ cells on the intensity of actinic light 680 (*1*) or 440 nm (*2*). F, fluorescence yield at 50 s after switching on the actinic light; F_M, maximum fluorescence yield under saturating intensity of actinic light. Data represents the mean value ± s.d. from three independent experiments; chlorophyll concentration, 10 μg/ml.
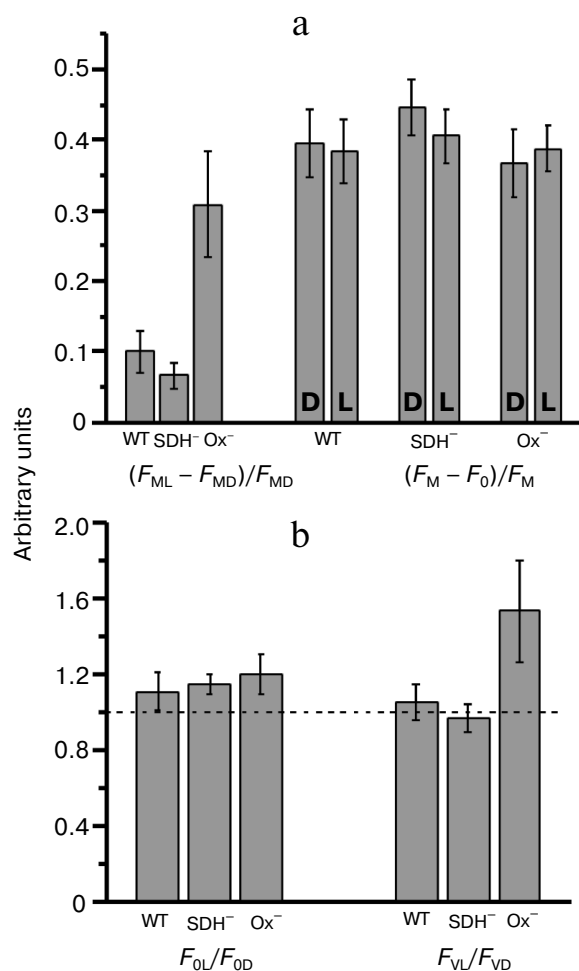
Fig. 6. Fluorescent parameters determined from the kinetic curves as presented in Fig. 4. a) Parameter indicating changes in the photosynthetic apparatus state $(F_{ML} - F_{MD})/F_{MD}$ and PSII quantum yield $(F_M - F_0)/F_M$ before (D) and after (L) illumination with actinic light 680 nm (70 µmol·m^{-2}·s^{-1}, 1 min) in wild-type (WT) and mutant SDH$^-$ and Ox$^-$ cells. b) Ratios of the initial (F_{0L}/F_{0D}) and variable (F_{VL}/F_{VD}) fluorescence levels before and after actinic illumination. The diagrams were plotted using mean values of parameters ± s.d. of 5-7 independent experiments.

content of PSII reaction centers in all cells (based on the variable fluorescence, Fig. 1d). The higher rate of the P700$^+$ re-reduction in the Ox$^-$ mutant was accompanied by a decrease in the variable fluorescence yield (phase I) just after phase J. Upon additional continuous 440-nm light, the variable fluorescence time course of Ox$^-$ cells became similar to those of WT and SDH$^-$ mutant (Fig. 7c). The kinetics of the redox reactions of P700 in all types of cells were the same under additional continuous 440-nm illumination (Fig. 7d). Thus, pulse-induced 620-nm light (predominantly absorbed by PBS) promoted the cyclic pathway around PSI and led to partial inactivation of PSII, while addition of continuous blue illumination (predominantly absorbed by chlorophyll) increased the rates of linear electron transport and PSII quantum efficiency in the Ox$^-$ mutant cells.

DISCUSSION

Our comparative investigation of variable and 77K fluorescence of dark-adapted *Synechocystis* WT and mutants revealed State 2 of the photosynthetic apparatus in Ox$^-$ mutant with deficiency of terminal oxidases and State 1 in WT and the SDH$^-$ mutant lacking succinate dehydrogenase. Actinic illumination that primarily activates PSI (light 1 in the presence or absence of DCMU) was able to promote State 2 to State 1 transition in the Ox$^-$ mutant. State 1 was characterized by higher rates of linear electron transport, whereas State 2 was characterized by suppressed linear and enhanced cyclic electron transport around PSI. These results corroborate the previous hypothesis [8] that state transition in cyanobacteria can be controlled by the extent of cyclic electron transport around PSI.

The difference in the state of dark-adapted mutants (Ox$^-$ and SDH$^-$) was clearly evident from comparative analysis of PSII variable fluorescence and 77K emission spectra of *Synechocystis* mutants and the WT. Illumination of the Ox$^-$ mutant with white light (for 30 min) increased the yields of maximum (F_M) and variable fluorescence (F_V, Fig. 1), while these changes in WT and SDH$^-$ mutant were less pronounced. The low variable fluorescence yield in cyanobacteria in the presence of DCMU is common for State 2 of the photosynthetic apparatus [27, 41]. Therefore, low variable and 77K fluorescence yields (684 and 692 nm) in dark-adapted Ox$^-$ mutant, as compared with SDH$^-$ and WT (Figs. 1 and 3 and table), suggest that prior to illumination the Ox$^-$ mutant was in State 2, while the SDH$^-$ mutant and WT were predominantly in State 1. The exposure of DCMU-treated Ox$^-$ cells to actinic 680-nm or 440-nm light for 1 min induced a gradual increase in the variable fluorescence component to the typical level of the WT and SDH$^-$ mutant (Figs. 4 and 5a). Similar changes in the fluorescence kinetics were observed earlier in the wild type of the cyanobacteria *Cyanothece* sp. and were attributed to the transition from State 2 to State 1 [23]. Transition from State 2 to State 1 was well pronounced in Ox$^-$, but almost absent in *Synechocystis* WT and SDH$^-$ mutant (Figs. 4 and 5a). As state transitions depend on the redox state of the PQ pool [8, 18, 19], our data may indicate a difference in the redox state of the PSII acceptor side between Ox$^-$ and WT and SDH$^-$ mutant. This is further supported by the analysis of the fluorescence induction curve (the ratio of the complementary area above the curve in the presence of DBMIB to that in the presence of DCMU), which indicated a more reduced PQ pool in the Ox$^-$ mutant compared to WT and SDH$^-$ (Fig. 2).

Low PSII fluorescence yield in the Ox$^-$ mutant correlated with high rates of P700$^+$ dark reduction (while illuminating with 730 nm light) and P700$^+$ re-reduction during the first 200 ms (using 620-nm light) (Figs. 1, 7a, and 7b). Considering the same relative content of PSII reaction centers in all cell types (Fig. 1d), the rapid P700$^+$
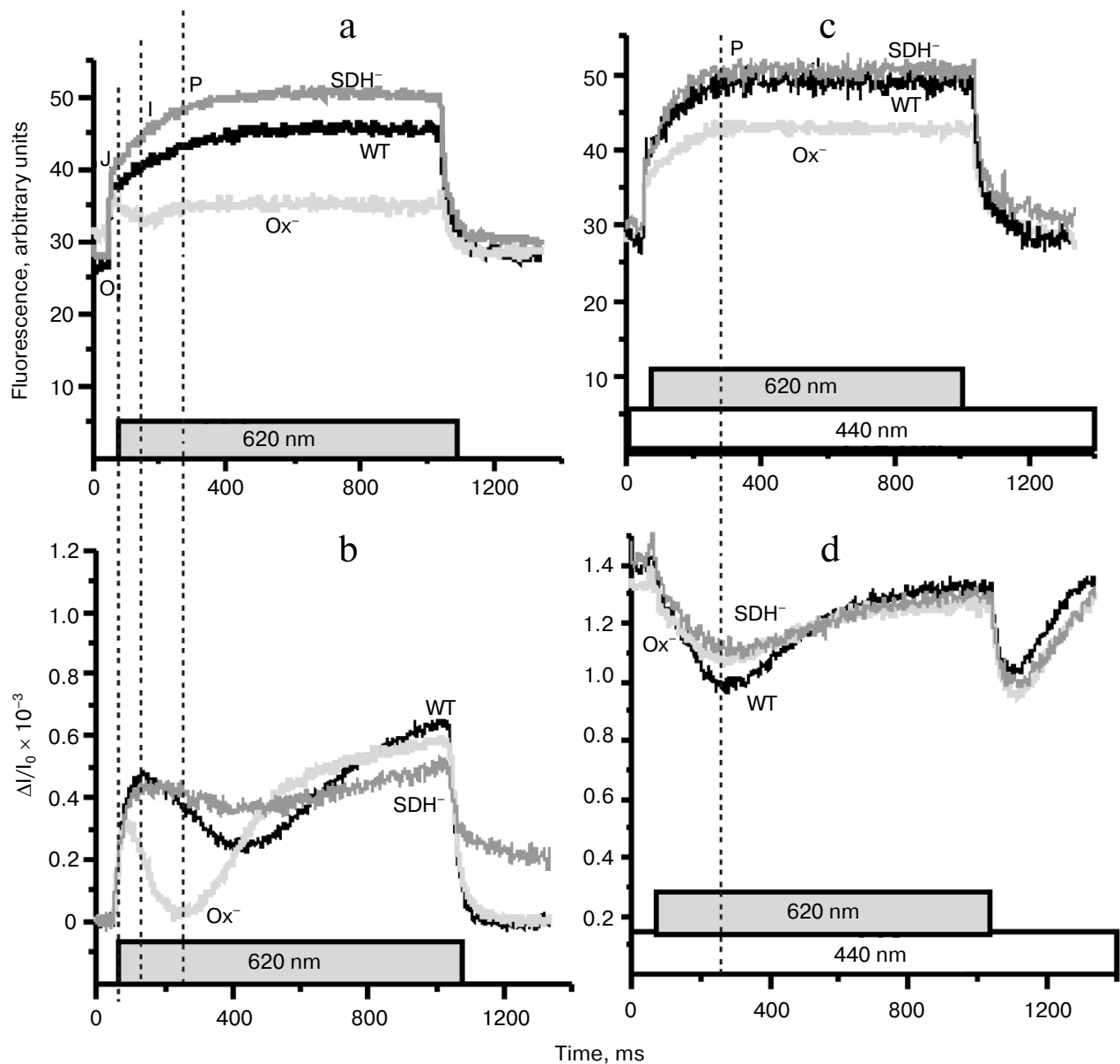
Fig. 7. Kinetics of variable fluorescence (a, c) and photoinduced absorption changes of P700 (b, d) in dark-adapted *Synechocystis* cells of wild type (WT, black) and mutants Ox⁻ (Ox⁻, light gray) and SDH⁻ (SDH⁻, gray) after incubation in the dark for 2 h. The experiments were carried out in the absence of DCMU. a, b) Kinetics were measured with 620-nm actinic light (300 $\mu mol \cdot m^{-2} \cdot s^{-1}$, 1 s) only; c, d) kinetics were measured with 620-nm actinic light against the background of continuous 440-nm light (70 $\mu mol \cdot m^{-2} \cdot s^{-1}$); O-J-I-P, fluorescence phases. Each curve represents an average of three curves obtained in three independent experiments; chlorophyll concentration, 5 $\mu g/ml$.

re-reduction during the first 200 ms of illumination in the Ox⁻ mutant may indicate enhanced cyclic electron transport, caused by the reduced PQ pool and, probably, by FNR inactivation during long dark adaptation.

There was a decrease in the fluorescence yield (I-phase of fluorescence induction) just after phase J and appearance of I-phase under additional continuous 440-nm light in dark-adapted Ox⁻ cells, in contrast to the WT and the SDH⁻ mutant cells (Figs. 7a and 7c). A dip beyond the J-level in fluorescence induction is thought to be due to a transient limitation on the donor side associated with P680⁺ formation, while the appearance of the I-

and P-phases may reflect transient reduction of the PSI acceptor side [43, 46]. Thus, the absence of I-phase in Ox⁻ mutant might reflect a limitation on the PSII donor side, while an increase in the variable fluorescence yield under additional continuous blue illumination may be a sign of acceleration of linear electron transport and reduction of all electron carriers in the electron transport chain from PSII down to the PSI acceptor side (Fd).

It is likely that in *Synechocystis* the low activity of FNR after prolonged dark adaptation prevented Fd re-oxidation under pulsed "phycobilisome" (620 nm) light. Under these conditions, the Ox⁻ mutant has a reduced PQ

a

Ox⁻

b

SDH⁻
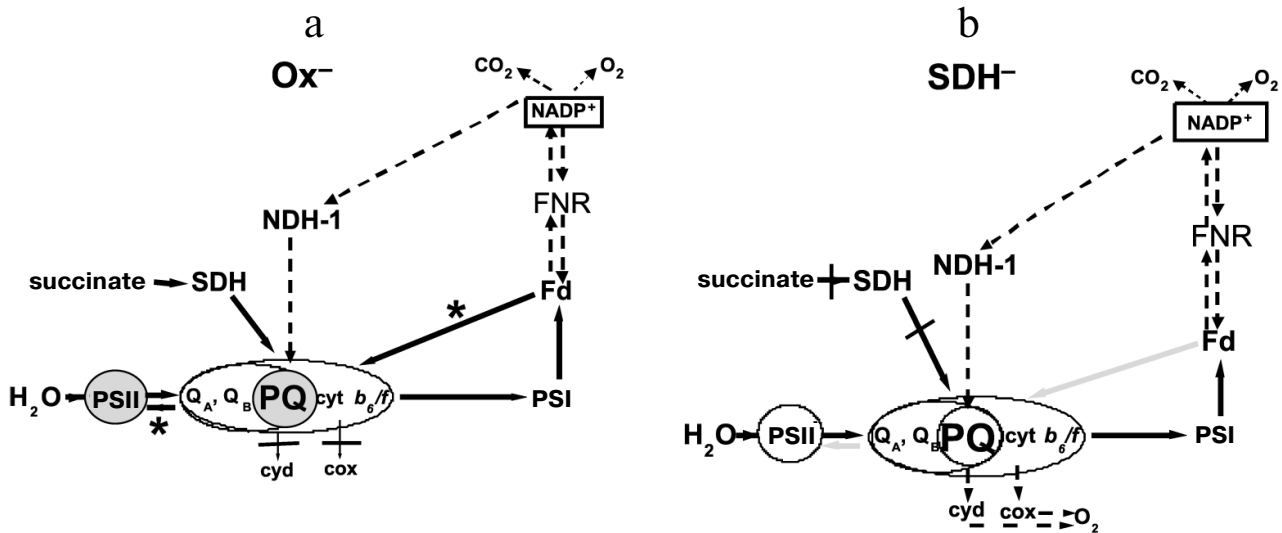
Electron transport pathways in dark-adapted Ox⁻ (a) and SDH⁻ (b) mutants of *Synechocystis* under pulsed light (620 nm, 300 μmol·m⁻²·s⁻¹). a) **PQ** on gray background is the reduced PQ pool, **PSII** on gray background is the inactivated PSII. Black arrows with asterisks denote reversible reactions, running with high rate, resulting in PSII inactivation. b) **PQ** on light background is oxidized PQ pool, **PSII** on light background is active PSII, as in WT. Gray arrows denote reversible reactions, running with rates that are insufficient for PSII inactivation. Dashed arrows denote slow reactions. Cyd and cox (CtaI) are terminal oxidases

Scheme

pool and high rates of cyclic electron transport around PSI and/or charge recombination. This ultimately decreased the rate of Q_A re-oxidation both under light flashes and during the dark intervals and might affect PSII activity (Scheme, panel (a)). Under additional continuous blue light, dark intervals were replaced by low illumination, which could not induce rapid cyclic electron transport around PSI, thus promoting Q_A^- and Q_B^- re-oxidation. We suggest the different effect of light 1 and light 2 on PSII activity in our experiments depends both on the light regime and on the different size of the light-harvesting antenna in PSI and PSII. Figure 5b shows that 680-nm light (partly absorbed by PBS) is twice as efficient as 440-nm light (absorbed by chlorophyll) in inducing PSII fluorescence yield rise. These data may be explained by the low PSII/PSI ratio and smaller chlorophyll *a* antenna size of PSII in cyanobacteria; PBS markedly increase PSII effective absorption cross-section, thus maintaining an overall balanced absorption of light and electron transport between the two photosystems [12, 13].

Inhibition of the linear electron transport on the acceptor side of PSII might result in reversible inactivation of the PSII donor side [43, 47-49]. Accumulation of reduced Q_A might cause quenching of PSII reaction center fluorescence as a result of charge recombination between Q_A^- and P680⁺ [43, 47-49]. It was demonstrated that the PSII inactivation rate in thylakoids was higher under exposure to a series of light flashes as compared with exposure to continuous light with equivalent total energy [50, 51]. The authors of [50, 51] suggest that during the dark interval between the flashes there was back electron transfer from the quinone acceptors to P680⁺, which was possibly accompanied by the non-radiative charge recombination with the S-states of the PSII donor side [51]. It was proposed that the lowering of 77K fluorescence yield of PSII (at 692 nm) in some higher plant species under high light treatment resulted from an increase in non-radiative energy dissipation during reversible photoinhibition [52]. In dark-adapted Ox⁻ mutant, we observed a low 77K fluorescence yield at 692 nm, which markedly increased after illumination with low white light (table and Fig. 3b). In WT, the 77K fluorescence yield at 692 nm slightly increased, and in the SDH⁻ mutant, it did not increase at all after illumination with white light (table and Fig. 3).

State 2 to State 1 transition is accompanied by movement of PBS [20, 21]. In the Ox⁻ mutant in the presence of DCMU, the state transition is evident from a 15-20% increase in the initial fluorescence (F_0) emitted predominantly by PBS (under 650-nm measuring light) and a 50-60% increase in the variable fluorescence component (F_V) originated from the PSII core (Fig. 6b). A correlation between the redox state of Q_A and movement of PBS during state transitions in *Synechocystis* was previously reported [53]. Taking into account greater sensitivity of PSII reaction centers to DCMU in the Ox⁻ mutant in State 1 in comparison to State 2, we suggest that movement of PBS during state transitions may be induced by changes in PSII reaction center activity (probably, due to Q_A/Q_B redox potential changes). This process may be associated with structural modification of the relative position of D_1 and D_2 PSII proteins and PBS complexes.

Thus in the dark-adapted Ox⁻ mutant, when the photosynthetic state is probed with phycobilin-absorbed pulsed light (620 nm), the reduced PQ pool and, probably, FNR inactivation could result in the shift of dynamic equilibrium between the PQ pool and Q_B site to a more reduced state of Q_B. This slows Q_A^- re-oxidation and, in turn, affects PSII activity, including suppression of the donor side and cooperative changes in the dynamics of D_1 and D_2 proteins and PBS conformation (Scheme, panel (a)). As in dark-adapted WT and SDH⁻ mutant, the PQ pool was more oxidized compared to the Ox⁻ mutant, and the 620-nm light could not arrest Q_A^- re-oxidation and following Q_B and PQ reduction even with low FNR activity (Scheme, panel (b)).

All our data indicated State 2 in the Ox⁻ mutant and State 1 in WT and the SDH⁻ mutant after incubation in the dark for 2 h. State 2 was characterized by low yield of variable and 77K fluorescence (at 692 nm). Based on our results, we propose that reversible PSII inactivation was caused by the high level of PQ pool reduction in State 2 in cyanobacteria. We also suggest that the reduction level of the PQ pool as well as the PSII effective absorption cross-section may be involved in regulating of state transitions via changes in the balance between cyclic and linear electron transport.

REFERENCES

1. Horton, P., Ruban, A. V., and Walters, R. G. (1996) Regulation of light harvesting in green plants, *Ann. Rev. Plant Physiol. Plant Mol. Biol.*, **47**, 655-684.
2. Karapetyan, N. V. (2007) Non-photochemical quenching of fluorescence in cyanobacteria, *Biochemistry* (Moscow), **72**, 1127-1135.
3. Bonaventura, C., and Myers, J. (1969) Fluorescence and oxygen evolution from *Chlorella pyrenoidosa*, *Biochim. Biophys. Acta*, **189**, 366-383.
4. Murata, N. (1969) Control of excitation transfer in photosynthesis. I. Light-induced change of chlorophyll *a* fluorescence in *Porphyridium cruentum*, *Biochim. Biophys. Acta*, **172**, 242-251.
5. Fork, D. C., and Satoh, K. (1983) State I–state II transitions in the thermophilic blue-green alga (cyanobacterium) *Synechococcus lividus*, *Photochem. Photobiol.*, **37**, 421-427.
6. Allen, J. F. (2003) State transitions—a question of balance, *Science*, **299**, 1530-1532.
7. Allen, J. F., Bennett, J., Steinback, K. E., and Arntzen, C. J. (1981) Chloroplast protein phosphorylation couples plastoquinone redox state to distribution of excitation energy between photosystems, *Nature*, **291**, 25-29.
8. Mullineaux, C. W., and Allen, J. F. (1990) State 1–state 2 transitions in the cyanobacterium *Synechococcus* 6301 are controlled by the redox state of electron carriers between photosystems I and II, *Photosynth. Res.*, **23**, 297-311.
9. Allen, J. F. (1992) Protein phosphorylation in regulation of photosynthesis, *Biochim. Biophys. Acta*, **1098**, 275-335.
10. Tsinoremas, N. F., Hubbard, J. A. M., Evens, M. C. W., and Allen, J. F. (1989) P700 photooxidation in state 1 and state 2 in cyanobacteria upon flash illumination with phycobilin- and chlorophyll-absorbed light, *FEBS Lett.*, **256**, 106-110.
11. Mullineaux, C. W. (1992) Excitation energy transfer from phycobilisomes to photosystem I in a cyanobacterium, *Biochim. Biophys. Acta*, **1100**, 285-292.
12. Rakhimberdieva, M. G., Boichenko, V. A., Karapetyan, N. V., and Stadnichuk, I. N. (2001) Interaction of phycobilisomes with photosystem II dimers and photosystem I monomers and trimers in the cyanobacterium *Spirulina platensis*, *Biochemistry*, **40**, 15780-15788.
13. Melis, A., Mullineaux, C. W., and Allen, J. F. (1989) Acclimation of the photosynthetic apparatus to photosystem I or photosystem II light: evidence from quantum yield measurements and fluorescence spectroscopy of cyanobacterial cells, *Z. Naturforsch.*, **44c**, 109-118.
14. Mi, H., Endo, T., Schreiber, U., Ogawa, T., and Asada, K. (1992) Electron donation from cyclic and respiratory flows to the photosynthetic intersystem chain is mediated by pyridine nucleotide dehydrogenase in the cyanobacterium *Synechocystis sp.* PCC 6803, *Plant Cell Physiol.*, **33**, 1233-1237.
15. Howitt, C. A., Smith, G. D., and Day, D. A. (1993) Cyanide-insensitive oxygen uptake and pyridine nucleotide dehydrogenases in the cyanobacterium *Anabaena* PCC 7120, *Biochim. Biophys. Acta*, **1141**, 313-320.
16. Cooley, J. W., Howitt, C. A., and Vermaas, W. F. J. (2000) Succinate:quinol oxidoreductase in the cyanobacterium *Synechocystis* sp. strain PCC 6803: presence and function in metabolism and electron transport, *J. Bacteriol.*, **182**, 714-722.
17. Pils, D., and Schmetterer, G. (2001) Characterization of three bioenergetically active respiratory terminal oxidases in the cyanobacterium *Synechocystis* sp. strain PCC 6803, *FEMS Lett.*, **203**, 217-222.
18. Mullineaux, C. W., and Allen, J. F. (1986) The state 2 transition in the cyanobacterium *Synechococcus* 6301 can be driven by respiratory electron flow into the plastoquinone pool, *FEBS Lett.*, **205**, 155-160.
19. Mao, H.-B., Li, G.-F., Ruan, X., Wu, Q.-Yu, Gong, Y.-D., Zhang, X.-F., and Zhao, N.-M. (2002) The redox state of plastoquinone pool regulates state transitions via cytochrome b_6f complex in *Synechocystis* sp. PCC 6803, *FEBS Lett.*, **519**, 82-86.
20. Mullineaux, C. W., and Holzwarth, A. R. (1990) A proportion of photosystem II core complexes are decoupled from the phycobilisome in light-state 2 in the cyanobacterium *Synechococcus* 6301, *FEBS Lett.*, **260**, 245-248.
21. Mullineaux, C. W., Tobin, M. J., and Jones, G. R. (1997) Mobility of photosynthetic complexes in thylakoid membranes, *Nature*, **390**, 421-424.
22. Schluchter, W. M., Shen, G., Zhao, J., and Bryant, D. A. (1996) Characterization of psaI and psaL mutants of *Synechococcus* sp. strain PCC 7002: a new model for state transitions in cyanobacteria, *Photochem. Photobiol.*, **64**, 53-66.
23. Meunier, P. C., Colon-Lopez, M. S., and Sherman, L. A. (1997) Temporal changes in state transitions and photosystem organization in the unicellular, diazotrophic cyanobacterium *Cyanothece* sp. ATCC 51142, *Plant Physiol.*, **115**, 991-1000.
24. Ivanov, A. G., Krol, M., Sveshnikov, D., Selstam, E., Sandstrom, St., Koochek, M., Park, Y.-I., Vasil'ev, S.,

Bruce, D., Oquist, G., and Huner, N. P. A. (2006) Iron deficiency in cyanobacteria causes monomerization of photosystem I trimers and reduces the capacity for state transitions and the effective absorption cross section of photosystem I *in vivo*, *Plant Physiol.*, **141**, 1436-1445.

25. Zhang, R., and Zhao, J. X. J. (2009) The mobility of PSI and PQ molecules in *Spirulina platensis* cells during state transition, *Photosynth. Res.*, **99**, 107-113.

26. McConnell, M. D., Koop, R., Vasil'ev, S., and Bruce, D. (2002) Regulation of the distribution of chlorophyll and phycobilin-absorbed excitation energy in cyanobacteria. A structure-based model for the light state transition, *Plant Physiol.*, **130**, 1201-1212.

27. Huang, Ch., Yuan, X., Zhao, J., and Bryant, D. A. (2003) Kinetics analyses of state transitions of the cyanobacterium *Synechococcus* sp. PCC 7002 and its mutant strains impaired in electron transport, *Biochim. Biophys. Acta*, **1607**, 121-130.

28. Mi, H., Klughammer, Ch., and Schreiber, U. (2000) Light-induced dynamic changes of NADPH fluorescence in *Synechocystis* PCC 6803 and its *ndh*B-defective mutant M55, *Plant Cell Physiol.*, **41**, 1129-1135.

29. Cooley, J. W., and Vermaas, W. F. J. (2001) Succinate dehydrogenase and other respiratory pathways in thylakoid membranes of *Synechocystis* sp. strain PCC 6803: capacity comparisons and physiological function, *J. Bacteriol.*, **183**, 4251-4258.

30. Van Thor, J. J., Jeanjean, R., Havaux, M., Sjollema, K. A., Joset, F., Hellingwerf, K. J., and Matthijs, H. C. P. (2000) Salt shock-inducible photosystem I cyclic electron transfer in *Synechocystis* PCC6803 relies on binding of ferredoxin:NADP$^+$ reductase to the thylakoid membranes via its CpcD phycobilisome-linker homologous N-terminal domain, *Biochim. Biophys. Acta*, **1457**, 129-144.

31. Thomas, D. J., Thomas, J., Youderian, Ph. A., and Herbert, St. H. (2001) Photoinhibition and light-induced cyclic electron transport in *ndh*$^-$ and *psa0*$^-$ mutants of *Synechocystis* sp. PCC 6803, *Plant Cell Physiol.*, **42**, 803-812.

32. Finazzi, G., Rappaport, F., Furia, A., Fleischmann, M., Rochaix, J.-D., Zito, F., and Forti, G. (2002) Involvement of state transition in the switch between linear and cyclic electron flow in *Chlamydomonas reinhardtii*, *EMBO Rep.*, **3**, 280-285.

33. Barbagallo, R. P., Bergo, E., Barbato, R., and Forti, G. (2001) Photoinhibition of *Chlamydomonas reinhardtii* in state 1 and state 2, *J. Biol. Chem.*, **276**, 22251-22257.

34. Bolychevtseva, Y., Elanskaya, I. V., and Karapetyan, N. V. (2011) Regulation of cyclic electron transport through photosystem I in the mutant cells of the cyanobacterium *Synechocystis* sp. PCC 6803 devoid of respiratory dehydrogenases, *Biochemistry* (Moscow), **76**, 427-437.

35. Howitt, C. A., Cooley, J. W., Wiskich J. T., and Vermaas, W. F. J. (2001) A strain of *Synechocystis* sp. PCC 6803 without photosynthetic oxygen evolution and respiratory oxygen consumption: implications for the study of cyclic photosynthetic electron transport, *Planta*, **214**, 46-56.

36. Howitt, C. A., and Vermaas, W. F. J. (1998) Quinol and cytochrome oxidases in the cyanobacterium *Synechocystis* PCC 6803, *Biochemistry*, **37**, 17944-17951.

37. Rippka, R., Deruelles, J., Waterbury, J. B., Herdman, M., and Stanier, R. Y. (1979) Generic assignments, strain histories and properties of pure cultures of cyanobacteria, *J. Gen. Microbiol.*, **111**, 1-61.

38. Lichtenthaler, H. K. (1987) Chlorophylls and carotenoids: pigments of photosynthetic biomembranes, in *Methods in Enzymology*, Vol. 148 (Colowick, S. P., and Kaplan, N. O., eds.) Academic Press Inc., San Diego, pp. 350-382.

39. Schreiber, U., Schliwa, U., and Bilger, W. (1986) Continuous recording of photochemical and non-photochemical chlorophyll fluorescence quenching with a new type of modulation fluorometer, *Photosynth. Res.*, **10**, 51-62.

40. Schreiber, U., Klughammer, C., and Neubauer, C. (1988) Measuring P700 absorbance changes around 830 nm with a new type of pulse modulation system, *Z. Naturforsch.*, **43c**, 686-698.

41. Mullineaux, C. W., and Allen, J. F. (1988) Fluorescence induction transients indicate dissociation of photosystem II from the phycobilisome during the State-2 transition in the cyanobacterium *Synechococcus* 6301, *Biochim. Biophys. Acta*, **934**, 96-107.

42. Berry, S., Schneider, D., Vermaas, W. F. J., and Roegner, V. (2002) Electron transport routes in whole cells of *Synechocystis* sp. strain PCC 6803: the role of the cytochrome *bd*-type oxidase, *Biochemistry*, **41**, 3422-3429.

43. Zhu, X.-G., Govindjee, Baker, N. R., d'Sturler, E., Ort, D. R., and Long, S. P. (2005) Chlorophyll a fluorescence induction kinetics in leaves predicted from a model describing each discrete step of excitation energy and electron transfer associated with photosystem II, *Planta*, **223**, 114-133.

44. Toth, S. Z., Schansker, G., and Strasser, R. J. (2007) A non-invasive assay of the plastoquinone pool redox state based on the OJIP-transient, *Photosynth. Res.*, **93**, 193-203.

45. Tsimilli-Michael, M., Stamatakis, K., and Papageorgiou, G. C. (2009) Dark-to-light transition in *Synechococcus* sp. PCC 7942 cells studied by fluorescence kinetics assesses plastoquinone redox poise in the dark and photosystem II fluorescence component and dynamics during state 2 to state 1 transition, *Photosynth. Res.*, **99**, 243-255.

46. Schansker, G., Toth, S. Z., and Strasser, R. J. (2006) Dark recovery of the Chl *a* fluorescence transient (OJIP) after light adaptation: the qT-component of non-photochemical quenching is related to an activated photosystem I acceptor side, *Biochim. Biophys. Acta*, **1757**, 787-797.

47. Van Wijk, K. J., and Van Hasselt, Ph. R. (1993) Photoinhibition of photosystem II *in vivo* is preceded by down-regulation through light-induced acidification of the lumen: consequences for the mechanism of photoinhibition *in vivo*, *Planta*, **189**, 359-368.

48. Ivanov, A. G., Sane, P. V., Hurry, V., Oquist, G., and Huner, N. P. A. (2008) Photosystem II reaction centre quenching: mechanisms and physiological role, *Photosynth. Res.*, **98**, 565-574.

49. Vass, I., and Cser, K. (2009) Janus-faced charge recombinations in photosystem II photoinhibition, *Trends Plant Sci.*, **14**, 200-205.

50. Keren, N., Berg, A., Van Kan, P. J. M., Levanon, H., and Ohad, I. (1997) Mechanism of photosystem II photoinactivation and D1 protein degradation at low light: the role of back electron flow, *Proc. Natl. Acad. Sci. USA*, **94**, 1579-1584.

51. Ohad, I., Berg, A., Berkowicz, S. M., Kaplan, A., and Keren, N. (2011) Photoinactivation of photosystem II: is there more than one way to skin a cat? *Physiol. Plant.*, **142**, 79-86.

52. Demmig, B., and Bjorkman, O. (1987) Comparison of the effect of excessive light on chlorophyll fluorescence (77K) and photon yield of O_2 evolution in the leaves of higher plants, *Planta*, **171**, 171-184.

53. Ma, W., Mi, H., and Shen, Yu. (2010) Influence of the redox state of Q_A on phycobilisome mobility in the cyanobacterium *Synechocystis* sp. strain PCC6803, *J. Luminesc.*, **130**, 1169-1173.